Applied Physics Letters

A microcantilever of self-suspended carbon nanotube forest for material characterization and sensing applications

Cite as: Appl. Phys. Lett. **117**, 013101 (2020); https://doi.org/10.1063/5.0012533
Submitted: 02 May 2020 . Accepted: 14 June 2020 . Published Online: 06 July 2020

Mohab O. Hassan, Alireza Nojeh, and Kenichi Takahata

Applied Physics Letters ARTICLE scitation.org/journal/apl

A microcantilever of self-suspended carbon nanotube forest for material characterization and sensing applications

Cite as: Appl. Phys. Lett. **117**, 013101 (2020); doi: 10.1063/5.0012533
Submitted: 2 May 2020 · Accepted: 14 June 2020 ·
Published Online: 6 July 2020

Mohab O. Hassan,[1,2] Alireza Nojeh,[1,2,a)] and Kenichi Takahata[1,a)]

AFFILIATIONS

[1]Department of Electrical and Computer Engineering, University of British Columbia, Vancouver, British Columbia V6T 1Z4, Canada
[2]Quantum Matter Institute, University of British Columbia, Vancouver, British Columbia V6T 1Z4, Canada

[a)]**Authors to whom correspondence should be addressed:** alireza.nojeh@ubc.ca and takahata@ece.ubc.ca

ABSTRACT

This paper reports a laterally suspended microcantilever made entirely of a vertically aligned carbon nanotube (CNT) forest. The CNTs in a 1-mm-long cantilever, patterned using a post-growth microplasma technique, are preserved in their original alignment and structure, and are self-suspended only due to their entwined arrangement and internal interactions. This pure CNT forest cantilever is electrostatically actuated to characterize its resonance using a laser Doppler vibrometer, revealing a resonant frequency and quality factor of 7.95 kHz and 51.3, respectively, at room temperature. The measurement result fitted to a free vibrating microcantilever model indicates that the CNT forest, an anisotropic bulk material, has an in-plane Young's modulus of 3.8 MPa, which matches well with previously reported levels of the modulus. A preliminary test of the cantilever as a resonant-mode sensing device shows real-time temperature tracking, suggesting the device's potential for not only temperature sensing but also other sensing applications.

Cantilever structures are one of the most common mechanical elements used for sensing and actuation in micro-electro-mechanical systems (MEMS). Based on different transduction methods, micropatterned cantilevers have been used as label-free, sensitive, fast, and highly parallel sensors[1–3] offering a tremendous range of potential applications[1,4] including fluidic flow, temperature, gas, humidity, and mass sensing. The sensing principle in a cantilever relies on detecting changes in the mass[5,6] or the surface/bulk stress developed in the cantilever structure.[7] These factors can be measured, among many other properties, through the static deflection or the change in the resonant frequency of the cantilever.[8] Cantilever resonators change their resonant frequencies as a function of their material properties and geometrical dimensions.[8] This feature enables, besides their sensing applications, characterization of the material properties by shaping the material of interest into a cantilever form and probing its resonant frequency. For example, resonant cantilever models have been used to analyze the Young's modulus and tensile strength of complex materials.[9–14]

Carbon nanotubes (CNTs) have drawn great attention due to their unique material properties in electrical, mechanical, and other domains.[15–17] CNTs are known for their high tensile strength, flexibility, and conductivity. All these properties have made the CNT a promising candidate in numerous application areas.[16,17] CNTs can be synthesized in different forms. One of the most interesting of these with unique physical properties, such as mechanical anisotropy, is an array of vertically aligned CNTs, known as a CNT forest.[18–20] Leveraging those properties, CNT forests have been studied for diverse electronics and mechanical applications including MEMS. For instance, interconnects on a microchip,[21] switches/relays,[13,22] field-emission, thermionic, and photoemission electron sources,[18,23,24] tunable[25,26] and super-[27,28] capacitors, and many other applications have been enabled using this unique nanomaterial.

Designing CNT forest-based structures and devices requires knowledge of the mechanical properties, such as the Young's modulus of CNT forests in the first place. Due to the alignment of CNTs along one axis, CNT forests exhibit great anisotropy in various properties. Many of the mechanical characterization studies have relied on using a nanoindentation technique to compress a forest in the out-of-plane direction (along the CNTs' axis).[29,30] Out-of-plane values of the Young's modulus ranging from 30 to 300 MPa were measured depending on the number of contact sites between the nanotubes within a CNT forest.[29] Other studies have shown similar results for

the out-of-plane elastic modulus.[31–33] On the other hand, there are limited reports on the in-plane elastic modulus. Much lower values, in the range of 1–10 MPa, were found using other techniques such as a measurement of the lateral bending in a parallel-plate capacitor configuration and a varactor.[25,26] Microscale cantilevers based on CNT forests have been reported as well, but by either modifying their structure/composition[13] or simply growing the forest on cantilever-shaped substrates, creating a complex/composite structure.[34,35] Currently, there are no reports on cantilevers made entirely of CNT forests that are laterally held. The primary reason is that conventional, lithography-based approaches do not allow three-dimensional (3D) carving of the material.

In contrast, micro-electro-discharge machining (μEDM) has been shown as an effective precision technique for free-form patterning of grown CNT forests while maintaining their vertical alignment and density.[36] This microplasma-based technique has been used to etch a variety of electrically conductive materials with submicrometer precision.[37] The removal mechanism relies on controlled discharges with thermomechanical impacts produced between a microscopic electrode and a workpiece. These features have been applied to 3D patterning of CNT forests[36,38] to create electron emission,[39] mechanical switching,[40] and scanning probe devices.[41] All of the previously reported works on μEDM of CNT forests were conducted on the top surface of the forests, with one exception that showed shallow μEDM of CNT forests' sidewall in one orientation.[42] Alternatively, deep localized etching of CNT forests from the sidewall in multiple orientations will enable the fabrication of unique 3D structures in the forest material. In this paper, we report the fabrication of a laterally suspended pure CNT forest cantilever device, using 3D μEDM, for a study of in-plane elastic modulus of the material through characterizing the resonance. This study further applies the CNT forest cantilever and the measurement method to a preliminary investigation for temperature sensing application of the structure.

A CNT forest was grown on a 6×6-mm^2 chip of a highly doped Si substrate (resistivity 0.002–0.005 Ω cm) using hot-wall atmospheric pressure chemical vapor deposition. The growth catalyst on the Si substrate consisted of a 1-nm Fe layer with a 10-nm Al_2O_3 layer underneath. The growth process was as follows. In the degassing phase, Ar was first introduced at 300 sccm for 10 min at room temperature. Then, the annealing phase was initiated, where the Ar flow rate was decreased to 100 sccm and H_2 was introduced at 400 sccm for 20 min while ramping up the temperature to 750 °C. Finally, the growth phase started by introducing C_2H_4 at 100 sccm and setting the flow rates of Ar and H_2 to 300 sccm and 100 sccm, respectively. The time of the growth phase was chosen to be 40 min, which resulted in a growth height of 1 mm or taller for the CNT forests. This level of the height was needed to enable the fabrication of the suspended cantilever in the grown forest (to be explained in the next paragraph). A conductive adhesive (Silver Paste Plus 05063-AB, SPI supplies, PA, USA) was used for electrical connection to the CNT forest as required for the μEDM process.[43]

A CNT forest with ~1.5 mm of height on a Si chip was mounted on the μEDM system (EM203, SmalTec International, IL, USA) so that the forest's plane was parallel to the Z axis of the system [Fig. 1(a)]. The CNTs were removed from a sidewall of the forest, by feeding the 300-μm-diameter tool electrode along the Z axis while scanning it in the X-Y plane, to etch the middle section of the CNTs

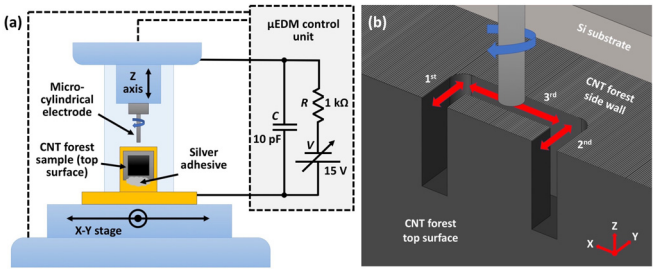

FIG. 1. Schematics of (a) the experimental setup for sideways 3D μEDM of the CNT forest (the CNTs are pointing out of the plane) and (b) a close-up of the patterning region showing the three removal steps used for the formation of the cantilever structure, whose thickness (Y) direction is parallel to the orientation of the individual CNTs in the forest, as illustrated.

while leaving the bottom and top sections attached to the substrate and suspended, respectively. The μEDM system with a relaxation-type pulse generator was programmed such that in the case of a short circuit event (that prevents proper removal), the X-Y scanning was stopped, and the electrode was retracted by 10 μm to clear the short circuit. Following the process conditions used in the previously reported studies on μEDM of CNT forests,[36] the process parameters were optimized for the lowest possible discharge energy that could sustain consecutive discharge pulses and minimize short circuit events. The discharge circuitry settings shown in Fig. 1(a) were used for this process, with the electrode's rotation and Z-feeding rate of 2000 rpm and 10 μm/min, respectively, and an X-Y scanning rate of 5 mm/min.

The CNT forest cantilever was directly fabricated at one of the four surface edges of the forest through three specific steps [Fig. 1(b)]. The first two steps were for removing the two sides of the cantilever and determining the width of the cantilever to be 1000 μm, and the third step was for defining the thickness of the cantilever and fully suspending the structure. The depth of the electrode feed in all three steps, which determined the length of the cantilever, was set to be 1000 μm. As-grown CNT forests, including the samples used in this study, inherently have certain height non-uniformity as well as curvatures at the surface edges.[43,44] This condition consequently led to a non-uniform thickness in the fabricated cantilever structure. We targeted the cantilever thickness of a few hundred micrometers through the discharge surface detection applied on the forest's top surface with respect to the third step. It should be noted that the top surface was not planarized prior to the cantilever patterning (although that could have been performed using a similar μEDM method)[43] because such planarization could result in a less reflective surface compared to the as-grown surface (as the planarization process removed the top layer of the CNT forest known as the crust layer formed by bent CNTs that made the surface more reflective),[38,45] which could then negatively impact the optical measurement of the cantilever's resonance to be conducted later.

High-aspect-ratio etching of the CNT forest from its side was demonstrated through the discharge process. The fabricated cantilever structure (Fig. 2) was measured to have lateral dimensions (length $\times$ width) of 992×960 μm^2, with its thickness ranging between 273 μm (fixed end) and 141 μm (free end). The micromachined lateral dimensions slightly differed from the programmed dimensions (1×1 mm^2) due to the presence of the discharge gap between the

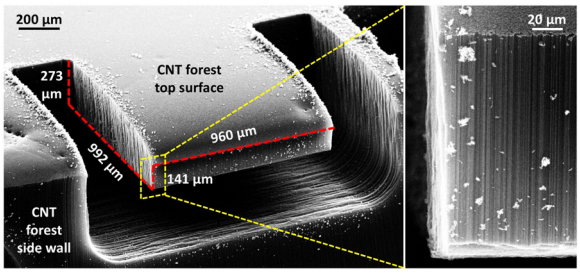

FIG. 2. A scanning electron microscope (SEM) image of the microcantilever patterned in a CNT forest. The inset is a close-up SEM of the free-end corner of the structure showing that the alignment of the individual CNTs was preserved after the patterning process.

electrode and the machined structure (potentially in combination with the effect of the carbon debris being stuck on the electrode to increase its effective diameter).[36] The process stability depends directly on the variation in the discharge gap. This variation along an entire side of the microcantilever was found to be ∼10 μm, which would have a minimal effect on its dimensions. Figure 2 (close-up) shows that the patterning process caused no apparent bending of CNTs in the vicinity of the removal area while preserving their original alignment in the structure. It should be emphasized that, contrary to other composite CNT forest cantilevers grown on a thin support layer of silicon or polysilicon,[34,35] the CNTs composing the cantilever fabricated here were supported and suspended on their own, without any other layer, due to the interactions of the nanotubes, likely with their physical entanglement (within the cantilever body and the top crust layer)[46] and possibly the van der Waals attractive forces acting among them.[47] This unique, pure CNT forest cantilever structure in turn simplifies modeling of its dynamic behavior in order to extract the mechanical properties of the material, the CNT forest, unlike in the reported composite cases.[34,35]

For mechanical resonant testing, a 200-μm-thick stainless-steel sheet, which served as the counter electrode for electrostatic actuation of the patterned forest cantilever, was fixed on alumina spacers above the cantilever at a distance of ∼320 μm (Fig. 3). The overlap between the cantilever structure and the stainless-steel electrode was adjusted manually to have a length of roughly 630 μm. The exposed length of the cantilever (∼370 μm) was necessary to facilitate the resonant frequency measurement with a laser Doppler vibrometer (LDV: MSA-500 Micro System Analyzer, Polytec, Waldbronn, Germany) that focused the probing laser onto the exposed part. No reflective coating on the cantilever was needed for this measurement.

Despite the measurement in air (which might pose squeeze-film/viscous damping effects in the cantilever actuation), a clear resonance was observed in the used setup. The quality (Q) factor and resonant frequency of the cantilever were measured to be 51.3 and 7.95 kHz, respectively, at room temperature (Fig. 4). (A higher harmonic peak was also observed at 16 kHz in some measurements, although this peak was relatively weak and non-repeatable.) The elastic modulus was extracted by fitting the measured resonant frequency data to a free vibrating microcantilever model.[10,11] The natural frequency of the cantilever, ω_n, is given by

$$\omega_n = \lambda_n^2 \sqrt{\frac{EI}{\overline{m}L^4}}, \quad (1)$$

$$\left(\lambda_1 \equiv 1.875, \lambda_2 \equiv 4.694, \lambda_3 \equiv 7.855, \text{and} \lambda_n \approx \frac{(2n-1)\pi}{2} \text{for} n > 3\right),$$

where E is the in-plane Young's modulus, I is the moment of inertia, $\overline{m}$ is the mass per unit length, L is the length of the cantilever, λ_n is the dimensionless natural frequency, and n is an integer number that represents the cantilever mode shape number. To determine the mass of the cantilever, we used a reported model suggesting that the mass per unit length of a single multiwall CNT (MWCNT) is given by $2.39 \times 10^{-21} \times D$ g/nm, where D is the diameter (in nm) of the MWCNT.[48] Based on SEM imaging, our CNT forests were estimated to have an areal density in the range of 1×10^{11}–1×10^{12} cm^{-2} and a MWCNT diameter on the order of ∼10 nm. Considering the mass of a single nanotube and assuming an average areal density value of 5×10^{11} cm^{-2}, we estimate 3.12×10^{-4} g/cm for the mass density per unit length for the cantilever. Fitting the measured resonance with the

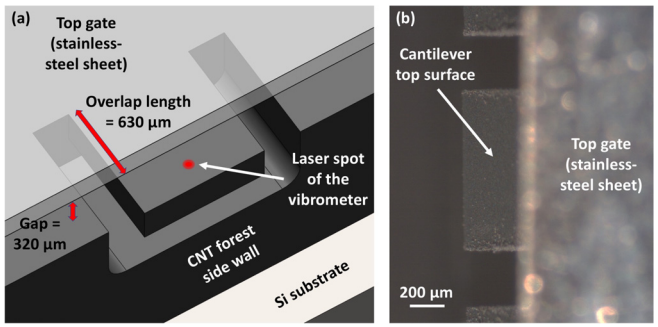

FIG. 3. The testing setup for the fabricated CNT-forest cantilever: (a) a schematic illustrating the setup used for electrostatic actuation and LDV measurement and (b) an optical microscope image showing the alignment of the top gate with respect to the CNT-forest cantilever.

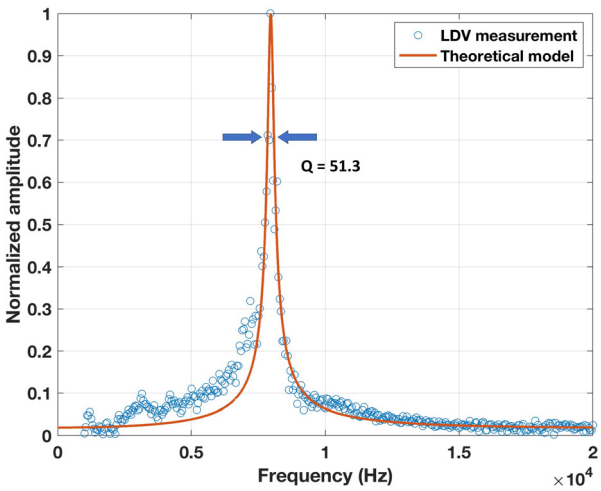

FIG. 4. The measured resonance of the CNT forest cantilever at 7.95 kHz plotted with the theoretical free vibrating microcantilever model.

calculated mass density to Eq. (1), the CNT forest structure was found to have an approximate in-plane Young's modulus of 3.8 MPa. This value matches very well with the range of the modulus values (1–10 MPa) reported for CNT forests.[26,34,35] This measurement and analysis reveal that the in-plane Young's modulus is one to two orders of magnitude smaller than the out-of-plane modulus (ranging from 30 to 300 MPa).[29–31] The reason behind this characteristic is that the entire forest cantilever structure is only held by the individual CNTs' interactions, such as their physical entanglements along with the van der Waals attraction forces acting among them, which could collectively bind them together to laterally suspend them in the form of the forest cantilever.

The study of the CNT forest resonator was extended in order to explore its potential for sensing applications. The temperature response of the resonance was characterized, in real time, by gradually heating the device (on a hotplate, up to 120 °C) while recording the local temperature of the cantilever using a thermographic camera (VarioCAM, Jenoptik, Jena, Germany). As shown in Fig. 5 which plots the measured results, the resonant frequency was found to decrease monotonically with increasing temperature. The frequency dependence on temperature appears to exhibit an approximate linear relationship with a coefficient of ∼−2.3 Hz/°C. While this needs further investigation on the exact phenomena involved in this dependence, one potential factor is a decrease in the in-plane Young's modulus or stiffness of the cantilever structure as a whole with temperature. The Young's modulus of the MWCNTs, entangled to constitute this entire structure, was reported to decrease with temperature (e.g., theoretically up to 9% with temperature increase from 100 K to 1200 K),[49,50] which could have partly contributed to a reduction in the cantilever's stiffness and, thus, the measured decrease in the resonant frequency. The obtained result is believed to represent a unique demonstration of the use of a CNT forest for resonance-based sensing at this point. This outcome, along with the common favorable features of the resonant sensing principle such as high sensitivity, large dynamic range, high linearity, and potentially low power,[51] encourages further investigation of the CNT-forest cantilever device for temperature and potentially other sensing applications.

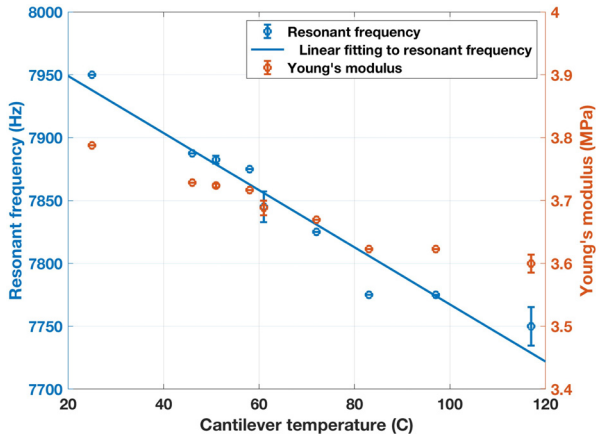

FIG. 5. The measured resonance dependency of the CNT forest cantilever on its temperature (left y-axis) and the corresponding change in the in-plane Young's modulus (right y-axis). Each data point is an average of five LDV frequency measurement scans.

In conclusion, we have reported a self-suspended pure CNT forest cantilever that was patterned through post-growth subtractive micromachining of pristine forest material. The entire cantilever was only supported through the interactions among individual CNTs constituting the cantilever's bulk structure. The Q factor and resonance frequency of the structure were experimentally characterized. Fitting the measured results to a resonator model, the in-plane Young's modulus of the CNT forest that formed the cantilever was found to be 3.8 MPa, significantly smaller than the reported out-of-plane modulus levels, as expected due to the particular anisotropic structure of the cantilever. Resonant-based real-time tracking of temperature using the cantilever device was demonstrated to suggest its potential for sensing applications.

The authors thank Dr. Edmond Cretu and Dr. Carlos Gerardo for providing access to and aid in measurement with the LDV. We acknowledge financial support from the Natural Sciences and Engineering Research Council of Canada (Grant Nos. SPG-P 478867, RGPIN-2017-04608, and RGPIN-2016-04252), the Canada Foundation for Innovation, and the British Columbia Knowledge Development Fund. This research was undertaken thanks in part to funding from the Canada First Research Excellence Fund, Quantum Materials and Future Technologies Program.

DATA AVAILABILITY

The data that support the findings of this study are available from the corresponding author upon reasonable request.

REFERENCES

[1]A. Boisen, S. Dohn, S. S. Keller, S. Schmid, and M. Tenje, Rep. Prog. Phys. **74**, 036101 (2011).
[2]K. S. Hwang, S.-M. Lee, S. K. Kim, J. H. Lee, and T. S. Kim, Annu. Rev. Anal. Chem. **2**, 77 (2009).
[3]S. Singamaneni, M. C. Lemieux, H. P. Lang, C. Gerber, Y. Lam, S. Zauscher, P. G. Datskos, N. V. Lavrik, H. Jiang, R. R. Naik, T. J. Bunning, and V. V. Tsukruk, Adv. Mater. **20**, 653 (2008).
[4]M. Hoffmann, H. Bezzaoui, and E. Voges, Sens. Actuators, A **44**, 71 (1994).
[5]T. Ono, X. Li, H. Miyashita, and M. Esashi, Rev. Sci. Instrum. **74**, 1240 (2003).
[6]J. Verd, A. Uranga, G. Abadal, J. L. Teva, F. Torres, J. López, F. Pérez-Murano, J. Esteve, and N. Barniol, IEEE Electron Device Lett. **29**, 146 (2008).
[7]M. Godin, V. Tabard-Cossa, Y. Miyahara, T. Monga, P. J. Williams, L. Y. Beaulieu, R. B. Lennox, and P. Grutter, Nanotechnology **21**, 075501 (2010).
[8]E. Finot, A. Passian, and T. Thundat, Sensors **8**, 3497 (2008).
[9]A. W. Leissa, *Vibration of Plates* (Ohio State University Columbus, 1969).
[10]C. E. Repetto, A. Roatta, and R. J. Welti, Eur. J. Phys. **33**, 1187 (2012).
[11]S. M. Heinrich and I. Dufour, in *Resonant MEMS* (Wiley-VCH, Weinheim, Germany, 2015), pp. 3–28.
[12]J. E. Sader, J. Appl. Phys. **84**, 64 (1998).
[13]Y. Hayamizu, T. Yamada, K. Mizuno, R. C. Davis, D. N. Futaba, M. Yumura, and K. Hata, Nat. Nanotechnol. **3**, 289 (2008).
[14]D. N. Hutchison, N. B. Morrill, Q. Aten, B. W. Turner, B. D. Jensen, L. L. Howell, R. R. Vanfleet, and R. C. Davis, J. Microelectromech. Syst. **19**, 75 (2010).
[15]R. Saito, G. Dresselhaus, and M. Dresselhaus, *Physical Properties of Carbon Nanotubes* (Imperial College Press, London, 1998).
[16]P. M. Ajayan and O. Z. Zhou, *Applications of Carbon Nanotubes* (Springer Berlin Heidelberg, 2001).
[17]R. H. Baughman, A. A. Zakhidov, and W. A. de Heer, Science **297**, 787 (2002).
[18]S. Fan, M. G. Chapline, N. R. Franklin, T. W. Tombler, A. M. Cassell, and H. Dai, Science **283**, 512 (1999).

[19]Y. Murakami, S. Chiashi, Y. Miyauchi, M. Hu, M. Ogura, T. Okubo, and S. Maruyama, Chem. Phys. Lett. **385**, 298 (2004).
[20]C. Wirth, S. Hofmann, and J. Robertson, Diamond Relat. Mater. **17**, 1518 (2008).
[21]T. Xu, Z. Wang, J. Miao, X. Chen, and C. M. Tan, Appl. Phys. Lett. **91**, 042108 (2007).
[22]M. Dahmardeh, M. S. M. Ali, T. Saleh, T. M. Hian, M. V. Moghaddam, A. Nojeh, and K. Takahata, Phys. Status Solidi A **210**, 631 (2013).
[23]A. Nojeh, MRS Bull. **42**, 500 (2017).
[24]P. Yaghoobi, M. Michan, and A. Nojeh, Appl. Phys. Lett. **97**, 153119 (2010).
[25]A. Arun, H. L. Poche, T. Idda, D. Acquaviva, M. F.-B. Badia, P. Pantigny, P. Salet, and A. M. Ionescu, Nanotechnology **22**, 025203 (2011).
[26]N. Olofsson, J. Ek-Weis, A. Eriksson, T. Idda, and E. E. B. Campbell, Nanotechnology **20**, 385710 (2009).
[27]D. N. Futaba, K. Hata, T. Yamada, T. Hiraoka, Y. Hayamizu, Y. Kakudate, O. Tanaike, H. Hatori, M. Yumura, and S. Iijima, Nat. Mater. **5**, 987 (2006).
[28]Y. Jiang, Q. Zhou, and L. Lin, in 2009 IEEE 22nd International Conference on Micro Electro Mechanical Systems (2009).
[29]C. M. Mccarter, R. F. Richards, S. D. Mesarovic, C. D. Richards, D. F. Bahr, D. Mcclain, and J. Jiao, J. Mater. Sci. **41**, 7872 (2006).
[30]H. Qi, K. Teo, K. Lau, M. Boyce, W. Milne, J. Robertson, and K. Gleason, J. Mech. Phys. Solids **51**, 2213 (2003).
[31]A. Cao, P. L. Dickrell, W. G. Sawyer, M. N. Ghasemi-Nejhad, and P. M. Ajayan, Science **310**, 1307 (2005).
[32]A. A. Zbib, S. D. Mesarovic, E. T. Lilleodden, D. Mcclain, J. Jiao, and D. F. Bahr, Nanotechnology **19**, 175704 (2008).
[33]C. P. Deck, J. Flowers, G. S. B. Mckee, and K. Vecchio, J. Appl. Phys. **101**, 023512 (2007).
[34]Y. Won, Y. Gao, M. A. Panzer, S. Dogbe, L. Pan, T. W. Kenny, and K. E. Goodson, Carbon **50**, 347 (2012).
[35]Y. Won, Y. Gao, M. A. Panzer, R. Xiang, S. Maruyama, T. W. Kenny, W. Cai, and K. E. Goodson, Proc. Natl. Acad. Sci. **110**, 20426 (2013).
[36]W. Khalid, M. S. M. Ali, M. Dahmardeh, Y. Choi, P. Yaghoobi, A. Nojeh, and K. Takahata, Diamond Relat. Mater. **19**, 1405 (2010).
[37]K. Takahata, *Micro-Electro-Discharge Machining Technologies for MEMS* (Intech Open Access Publisher, 2009).
[38]T. Saleh, M. V. Moghaddam, M. S. M. Ali, M. Dahmardeh, C. A. Foell, A. Nojeh, and K. Takahata, Appl. Phys. Lett. **101**, 061913 (2012).
[39]M. V. Moghaddam, M. S. Sarwar, Z. Xiao, M. Dahmardeh, K. Takahata, and A. Nojeh, in 2013 26th International Vacuum Nanoelectronics Conference (IVNC) (2013).
[40]M. Dahmardeh, M. V. Moghaddam, M. H. Tee, A. Nojeh, and K. Takahata, Appl. Phys. Lett. **103**, 231606 (2013).
[41]Z. Xiao, M. S. Sarwar, M. Dahmardeh, M. V. Moghaddam, A. Nojeh, and K. Takahata, Appl. Phys. Lett. **103**, 171603 (2013).
[42]Y. W. Zhu, C.-H. Sow, M.-C. Sim, G. Sharma, and V. Kripesh, Nanotechnology **18**, 385304 (2007).
[43]M. O. Hassan, A. Nojeh, and K. Takahata, ACS Appl. Nano Mater. **2**, 4594 (2019).
[44]M. Bedewy, B. Farmer, and A. J. Hart, ACS Nano **8**, 5799 (2014).
[45]N. Tomlin, A. Curtin, M. White, and J. Lehman, Carbon **74**, 329 (2014).
[46]L. Zhang, Z. Li, Y. Tan, G. Lolli, N. Sakulchaicharoen, F. G. Requejo, B. S. Mun, and D. E. Resasco, Chem. Mater. **18**, 5624 (2006).
[47]M. F. D. Volder, D. O. Vidaud, E. R. Meshot, S. Tawfick, and A. J. Hart, Microelectron. Eng. **87**, 1233 (2010).
[48]S. Esconjauregui, R. Xie, M. Fouquet, R. Cartwright, D. Hardeman, J. Yang, and J. Robertson, J. Appl. Phys. **113**, 144309 (2013).
[49]C.-L. Zhang and H.-S. Shen, Appl. Phys. Lett. **89**, 081904 (2006).
[50]Y. Zhang, X. Chen, and X. Wang, Compos. Sci. Technol. **68**, 572 (2008).
[51]D. Pinto, D. Mercier, C. Kharrat, E. Colinet, V. Nguyen, B. Reig, and S. Hentz, Procedia Chem. **1**, 536 (2009).